

POWER MANAGEMENT STRATEGY IN ISLANDED GRID DC MICROGRID

A.S.Valarmathy, Associate Profesor
Prince Shri Venkateshwara Padmavathy
Engineering College, Ponmar, Chennai-600127

Abstract— In addition to the production of renewable energy sources, Photovoltaic (PV) and wind turbines (WT), for instance, The energy storage system (ESS) is becoming a vital part of the energy storage system. Micro grids focused on renewables. In this article, Dual-active-bridge (DAB) bidirectional power-flowing capacity dc-dc converter, The broad range of soft-switching and ultra-fast dynamic characteristics are Adopted for multiple energy storage units (ESUs) to be combined for Balancing the flow of energy between renewable energy and The loads in the DC micro grids of an island. For the multiple energy storage device based on DAB, a communication-free power management scheme.

I. INTRODUCTION

A small-scale grid system based on the concept of smart grids was proposed [1]–[2] for small islands, mountains, industrial parks, and remote areas. Such a small-scale grid is called a micro grid (MG). MGs are classified based on the grid type into ac grid, dc grid, and hybrid grid. In recent years, interest in the dc MG system has gradually increased with the growth in the dc coupled subsystems such as photovoltaic, batteries, and LEDs. Noticeable benefits of the dc grid system are that there are no reactive powers, harmonics, and synchronization issues [3]–[4]. A typical dc MG system consists of renewable energy sources (RESs), local loads, an energy storage system (ESS), and a voltage source inverter (VSI), as shown in Fig. 1. The RESs are expected to steadily operate at the maximum power point (MPP) regardless of the ac utility grid condition. To balance the power difference between the RESs and local loads, the VSI in connection with the utility grid regulates the dc-bus voltage. The ESS is used to prevent power fluctuations caused by the stochastic characteristics of the RESs that may lead to the instability of the utility grid. Moreover, the ESS is indispensable for energy management tasks such as peak-cut, load shifting, and load leveling. Besides, the ESS should be able to act as a backup power source during a failure of the utility grid when islanded operation is required. During mode switching between the grid-connected mode and the islanded mode, a large transient phenomenon accompanied by oscillation and overshoot may appear because of a sudden failure of the utility grid. The mode switching should be one of the important considerations in the control strategies of the MG [5]–[8]. Several control strategies dealing with mode switching have been presented in [8]–[15]. A possible approach proposed in [11] is that the ESS takes charge of the dc-bus voltage regulation instead of the VSI in both modes, thereby avoiding the issue associated with mode switching.

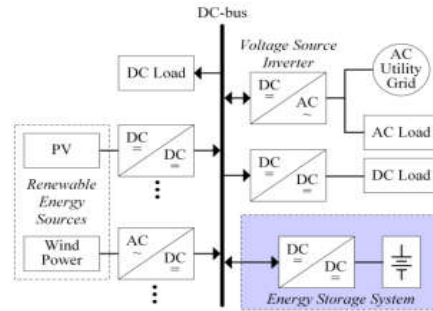


Fig. 1. Typical dc microgrid system.

However, in this approach, frequent charging/discharging cycles caused by unpredictable power fluctuations from the RESs and local loads can lead to a reduced battery lifetime [12]. Practically, most of the studies have proposed individual control loops for each mode [8], [12]–[14] although there exists an issue on mode switching. Coordinated control schemes presented in [14]–[15] are realized in a central controller. In this control scheme, all power conversion units in the MG are controlled by real time commands from the central controller with a high bandwidth communication link. However, the large distances among the power conversion units are an obstacle to establishment of the high bandwidth communication link. In addition, a communication failure can cause an inoperable condition of the MG. In [9] and [12], distributed control systems operating autonomously with a low bandwidth communication have been proposed to reduce the reliance on the communication with the central controller. This is commonly accepted as an efficient management method in MGs [17]–[18]. A mode switching strategy of the BDC for ESS is critically important to maintain a stable dc-bus voltage and a steady MPP tracking of RESs even under a failure of the utility grid. In [12]–[14], control schemes of the BDC have been realized with individual control loops which are generally implemented as proportional-integral (PI) compensators according to the control objective such as a dc-bus voltage, battery current, or battery voltage regulation. Fig. 2 shows concept of the conventional mode switching scheme where these two control loops can be interactively interchanged through the mode selector by a fault detector or a command from the central controller. This interchanging can lead to instability due to the transient response inherent in the control loop. Smooth transition between the control loops in Fig. 2 can be achieved by forcing the initial conditions of the inactive PI compensator to the output value of the active PI compensator. However, this approach may suffer from the chattering phenomenon in judging the operating mode. To increase the reliability, it is necessary to have a strategy that can achieve autonomous mode switching without depending on an external signal

from the fault detector or the central controller. In [9] and [19], the charging and discharging control loops are combined for autonomous mode switching. However, these methods do not deal with mode switching under the discharging condition. This paper proposes a control scheme of the BDC for the ESS to resolve the issue associated with the mode switching. In the proposed control scheme, control loops for dc-bus voltage, battery current, and battery voltage are combined by variable limiters, and switching of the control objective of the proposed control scheme is not only autonomous but also smooth, thereby reducing the reliance on the communication and enhancing the reliability of the system. Furthermore, an autonomous and smooth mode switching can be achieved under both charging and discharging conditions, which can contribute to efficient energy management in the grid-connected mode.

II. THE COMMUNICATION FREE POWER MANAGEMENT STRATEGY FOR THE MULTIPLE DAB-BASED ESS

In this Section, for the multiple DAB-based ESS, the communication-free power management strategy is proposed to maintain the dc-link voltage when the input voltage, the load condition and the power sharing performance of the ESS are varied. Moreover, the parameter design principle is presented. Further, the seamless hot swap operation of the ESU is proposed. In addition, the potential extension to low bandwidth high-level control system of the proposed strategy is presented.

A. The Proposed Communication -

Free Power Management Strategy for the DAB-Based ESS. In order to realize the flexible power transmission, the single-phase-shift (SPS) modulation method is the most popular modulation method for the DAB dc-dc converter. Thus, in this paper, the SPS modulation method is adopted, which can be illustrated in Fig. 2, where $S_{a1}\sim S_{a8}$ are the switching signals for the corresponding switches, $U_{ab\alpha}$ is the output voltage of the primary-side H Bridge, $U_{cd\alpha}$ is the output voltage of the secondary-side H Bridge, i_{La} is the inductance current, D_α is the phase-shift ratio and $T_{s\alpha}$ is the switching period of the α th DAB dc-dc converter for the α th ESU.

When the ESU injects power to the dc grid, the transferred power of the DAB module is assumed as positive, and when the ESU absorbs power from the dc grid, the transferred power of the DAB module is assumed as negative. According to Fig. 4, the transferred power under SPS modulation method can be expressed as, analysis and time-domain simulations are performed using Mat lab/Simulink

$$P_\alpha = \begin{cases} \frac{U_{in\alpha} U_{dc} D_\alpha (1-D_\alpha) T_{s\alpha}}{2n_\alpha L_\alpha} & (P_\alpha \geq 0) \\ -\frac{U_{in\alpha} U_{dc} D_\alpha (1-D_\alpha) T_{s\alpha}}{2n_\alpha L_\alpha} & (P_\alpha < 0) \end{cases} \quad (1)$$

Then, according to (1), the phase-shift ratio D_α can be calculated as,

$$D_\alpha = \begin{cases} \frac{1}{2} - \sqrt{1 - \frac{8L_\alpha P_\alpha}{n_\alpha U_{in\alpha} U_{dc} T_{s\alpha}}} & (P_\alpha \geq 0) \\ \frac{1}{2} + \sqrt{1 + \frac{8n_\alpha L_\alpha P_\alpha}{U_{in\alpha} U_{dc} T_{s\alpha}}} & (P_\alpha < 0) \end{cases} \quad (2)$$

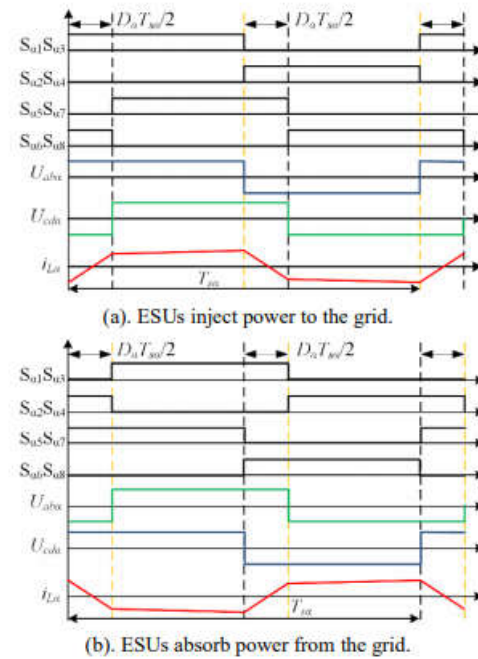


Fig. 2. The SPS modulation method of DAB converter for bidirectional power flowing conditions

Moreover, to implement the communication-free control performance, the droop control concept is adopted in this paper, and the desired dc-link voltage $U_{dc\alpha}$ for each ESU can be expressed as

$$U_{dc\alpha} = U_{nom} - \frac{P_\alpha}{k_\alpha P_T^*} = U_{nom} - \frac{P_\alpha}{k_\alpha U_{nom} i_o^*} \quad (3)$$

where k_α is the droop coefficient, U_{nom} is the nominal voltage of the dc grid, $P^* T$ is the total desired output power and $i^* o$ is the desired output current of the ESS. In (3), the total desired output power $P^* T$ is employed to unify the transferred power P_α of the α th ESU, and the desired output current $i^* o$ of the ESS can be expressed as,

$$i_o^* = \frac{U_{nom}}{R_{TE}} = \frac{U_{nom} i_o}{U_{dc}} \quad (4)$$

where R_{TE} is the total equivalent load resistor. In addition, based on the power control concept, the required transferred power for the α th DAB module can be shown as,

$$P_\alpha^* = \frac{U_{va} U_{nom} i_o}{U_{dc}} \quad (5)$$

ESS is calculated, and based on (1), the transferred power of each ESU can be obtained. Since the load current is adopted, the excellent dynamic response can be obtained by using the power-based control in this proposed communication-free power management strategy. Further, combining (3), the desired dc-link voltage $U_{dc\alpha}$ for each ESU can be obtained. Moreover, based on the power control concept, the required transferred power P_α^* for each ESU can be acquired by (5). In addition, combining Fig. 4 and (2), the phase-shift ratio D_α can be calculated for realizing the required transferred power for each ESU.

Since the input voltage is acted as the feedback value for each modulation structure, the required transferred power from the power-based control can be ensured even.

Then when the input voltage of DAB module is changed. Then, the fast dynamic performance can be achieved when the output voltage of energy storage component is changed. Importantly, in the modulation Part, other phase-shift modulation methods such as the dual-phase-shift modulation method, the extended phase-shift modulation method and the triple-phase shift modulation method can be employed for boosting the efficiency of the whole converter system since the transferred power is acted as the middle control value between the power-based control structure and the modulation structure. Therefore, based on the proposed communication-free power management strategy for ESS, the ultrafast dynamic response can be obtained to ensure the stability of the dc system.

In addition, since the control loop for each ESU contains the PI controller based on the droop control concept, which can boost the autonomy characteristic of the ESU, and it is easy to realize the hot swap of the ESU. In addition, according to (3), when the droop parameter of one ESU is reduced for smaller transferred power, other ESUs will share more power requirement with the same droop parameters, so the steady-state dc-link voltage will be close to the nominal dc-link voltage.

Conversely, the steady-state dc-link voltage will be away to the nominal dc-link voltage. B. The Design Principle of the PI Parameter and the Droop Coefficients. For DAB dc-dc converter, the relationship between the phase-shift ratio and the transferred power or current is similar in steady state condition or during transient process [20]. Thus, leakage inductances of these converters don't affect the dynamic performance, and DAB modules can be directly regarded as current sources.

Generally, when input voltage or load condition are changed, desired voltages $U_{dc\alpha}$ from the droop control structure can be treated as constant values. Then, the power-based control method for the multiple DAB-based ESS can be illustrated. Assuming ESUs are working on power balancing performance, the transfer function of each DAB module can be expressed as

$$H_a(s) = \frac{U_{nom} i_o}{m U_{dc}^2} \frac{k_{pa} s + k_{ia}}{s} \frac{1}{SC_{dc}} \approx \frac{i_o}{m U_{dc}} \frac{k_{pa} s + k_{ia}}{s} \frac{1}{SC_{dc}} \quad (6)$$

here m is the number of the ESU, k_{pa} is the proportionality coefficient and k_{ia} is the integral coefficient of the PI controller. According to (6), since DAB dc-dc converter is the first-order system with capacitive character, the phase margin always close to 90°. Then, in order to ensure the stability of DAB module, the cross-over frequency is set as the switching frequency f_{sa} . Moreover, assuming k_{pa} is ten times as k_{ia} , k_{pa} . Based on (7), k_{pa} is usually bigger than 100, and combining Fig. 8, the control system can provide a stable dc-link voltage. However, although oscillations of the dc-link voltage U_{dc} can be easily evitable with the dc-

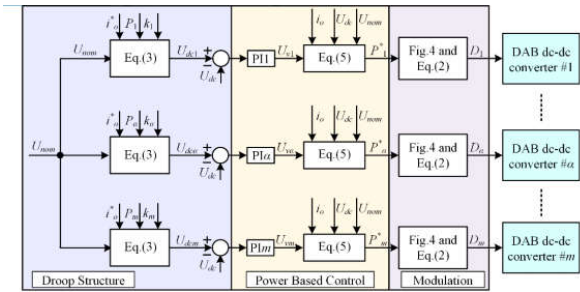


Fig.3. The communication-free power management strategy for multiple DAB-based ESS.

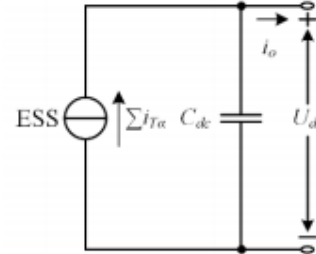


Fig.4. The simplified circuit of multiple DAB-based ESS

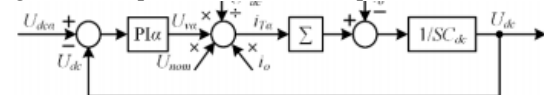


Fig.5. The power-based control scheme for the DAB dc-dc converter

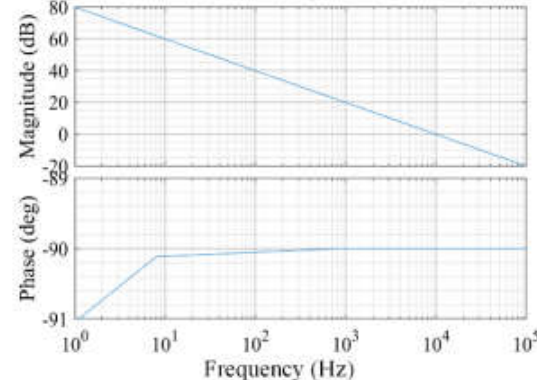


Fig.6. The bode diagram of the power-based control method for the DAB module.

link capacitor, there are obvious disturbances in phase-shift ratio with measurement noise since the power transferring range of DAB converter is limited. Thus, the disturbances ΔD_α of the phase-shift ratio caused by the measurement noises should also be treated as a criterion to evaluate the stability of the DAB dc-dc converter. Then, combining (2), (5) and Fig. 5,

$$\Delta D_\alpha \approx \sqrt{1 - \frac{8n_\alpha L_\alpha [U_{av} + (k_{pa} + k_{ia}) U_{dcmn}] U_{nom} i_o}{U_{ina} U_{dc}^2 T_{as}}} - \sqrt{1 - \frac{8n_\alpha L_\alpha U_{av} U_{nom} i_o}{U_{ina} U_{dc}^2 T_{as}}} \quad (8)$$

$$(k_{pa} + k_{ia}) \approx \left| \frac{\Delta D_\alpha}{U_{dcmn}} \sqrt{1 - \frac{8n_\alpha L_\alpha U_{av} U_{nom} i_o}{U_{ina} U_{dc}^2 T_{as}}} \frac{U_{ina} U_{dc}^2 T_{as}}{4U_{nom} i_o n_\alpha L_\alpha} \right| \quad (9)$$

Further, assuming the maximum phase-shift ratio disturbance is $\Delta D_{a\max}$, (9) can also be expressed as,

$$(k_{pa} + k_{ia}) \leq \left| \frac{\Delta D_{a\max}}{U_{dcmn}} \sqrt{1 - \frac{8n_\alpha L_\alpha U_{av} U_{nom} i_o}{U_{ina} U_{dc}^2 T_{as}}} \frac{U_{ina} U_{dc}^2 T_{as}}{4U_{nom} i_o n_\alpha L_\alpha} \right| \quad (10)$$

Then, k_{ia} can be designed as tenth of k_{pa} since transferred power in steady-state condition is mainly depended on the feedback values, and (10) can be further expressed as,

$$\begin{cases} k_{pa} \leq \frac{\Delta D_{a\max}}{U_{dcmn}} \sqrt{1 - \frac{8n_\alpha L_\alpha U_{av} U_{nom} i_o}{U_{ina} U_{dc}^2 T_{as}}} \frac{U_{ina} U_{dc}^2 T_{as}}{4U_{nom} i_o n_\alpha L_\alpha} \\ k_{ia} \leq \frac{\Delta D_{a\max}}{10U_{dcmn}} \sqrt{1 - \frac{8n_\alpha L_\alpha U_{av} U_{nom} i_o}{U_{ina} U_{dc}^2 T_{as}}} \frac{U_{ina} U_{dc}^2 T_{as}}{4U_{nom} i_o n_\alpha L_\alpha} \end{cases} \quad (11)$$

In addition, the droop coefficient k_α is also the main control parameter in the communication-free power management strategy for power sharing performance of different ESUs. Based on the droop control concept, the voltage error ΔU_{dc} between the steady-state dc-link voltage U_{dc} and the nominal dc-link voltage U_{nom} is given by

$$\Delta U_{dc} = U_{nom} - U_{dc} = \frac{I_\alpha}{k_\alpha U_{nom} i_o} \quad (12)$$

When the power balancing performance is realized among different ESUs for the ESS, (12) can be further illustrated as

$$\Delta U_{dc} = \frac{1}{k_\alpha m} \quad (13)$$

Then, assuming the allowed maximum voltage error is $\Delta U_{dc\max}$, the droop coefficient k_α can be further expressed as,

$$k_\alpha \geq \frac{1}{m \Delta U_{dc\max}} \quad (14)$$

Notably, the allowed maximum voltage error $\Delta U_{dc\max}$ between the nominal dc-link voltage and the steady dc-link voltage should be bigger than the measurement noise U_{dcmn} . Then, the droop coefficient k_α can be further expressed as,

$$\frac{1}{m \Delta U_{dc\max}} \leq k_\alpha < \frac{1}{m U_{dcmn}} \quad (15)$$

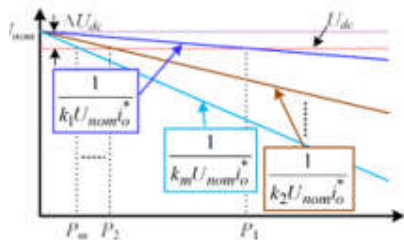


Fig. 7. The regulation characteristic of the droop control in the communication-free power management strategy

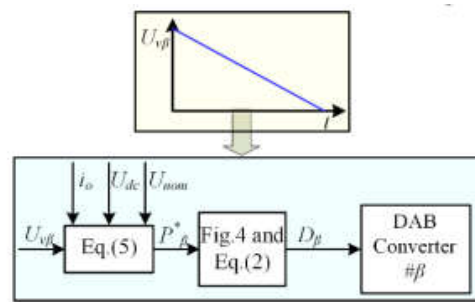


Fig. 8. The plug-out process of the β th DAB-based ESU

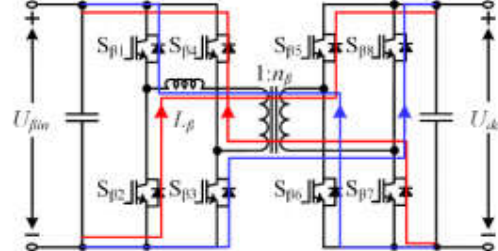


Fig. 9. The circuit condition for consuming the storage energies in the inductances of the DAB dc-dc module.

Usually, in order to reduce the impact of the measurement noise obviously, (15) can be further expressed for the practice application

$$\frac{1}{m \Delta U_{dc\max}} \leq k_\alpha \leq \frac{1}{2m U_{dcmn}} \quad (16)$$

In addition, when the β th DAB-based ESU should be plugged out, the transferred power of this ESU should become zero firstly, and the plug-out process of this DAB-based ESU can be shown in Fig. 8, where the virtual output voltage $U_{v\beta}$ is gradually reduced to zero, and the transferred power of this ESU will be decreased to zero. Notably, this plugged-out ESU can be treated as load by other ESUs, and the β th DAB-based ESU will not control the dc-link voltage actively. Moreover, with the feedback value of the load current and the input voltage, this plugged-out ESU can offer the timely response when the load condition or input voltage are changed.

Thus, the robustness of the dc-link voltage can be ensured during the plug-out process of the ESU. Then, when the transferred power of the β th DAB-based ESU is become zero, the storage energy in the leakage inductance of the transformer should be consumed before plug-out action, and with the parallel diodes, these storage energies can transfer to the ESU and the dc-link bus by turning off all the switches. The corresponding circuit can be shown as Fig. 9.

Further, when the inductance current is become zero, there is not exchanging power between the ESU and the dc-link bus and flowing current in DAB dc-dc module, and the β th DAB-based ESU can be completely plugged-out from the ESS. According to (13), number of the ESUs is decreased, the voltage error between the actual dc-link voltage and the nominal voltage is preferred to be bigger. Thus, when the steady-state condition is obtained again,

the actual dc-link voltage will be a little away from the nominal dc-link voltage in the isolated dc micro grid. D. The Power

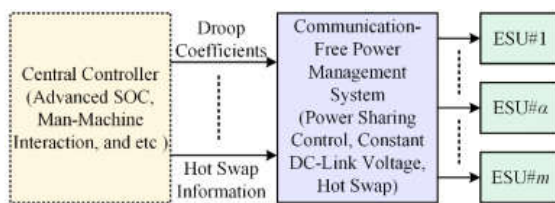


Fig. 10. The potential system structure for the proposed communication-free power management strategy with low bandwidth high-level central controller.

By presenting different droop coefficients for different the state of charge (SOC) conditions of the energy storage equipment, the balanced SOC performance among different ESUs can be obtained through relatively long-time fuzzy regulation function [36-37]. However, sometimes, higher requirement of the SOC performance of the ESUs should be provided, and the centralized man-machine interaction system of the ESS may be required. Then, a high-level control system may be required, and the potential system structure for the communication-free power management strategy with high level central controller can be shown in Fig. 10 . A cyber layer, comprised of all communication links, is spanned among the sources to facilitate data exchange. This is a sparse communication network with at least a spanning tree and is also chosen such that in case of any link failure the remaining network still contains a spanning tree.

In Fig. 10, the central controller can be employed to ensure advanced SOC of different ESUs and provide good manmachine interaction system of the whole ESS. Importantly, based on the proposed communication-free power management strategy, the high-level central control system will not affect the dc-link voltage, and when the ESU is plugged in or plugged out, the reprogramming operation is not required since each ESU has self-regulating ability with the integrated close-loop structure containing t

III. CONCLUSION

In this paper, a communication-free power management strategy with seamless hot swap ability is proposed, which can combine the droop control concept, the dynamic optimization control and the all kinds of phase-shift modulation methods for the multiple DAB-based energy storage system. Based on simulation and experimental verifications of the proposed strategy, the conducted studies in this work can lead to the following conclusions:

- 1). Based on the proposed communication-free power management strategy, the dc-link voltage can be kept stable when the output voltage of the energy storage equipment and the load condition of the multiple DAB-based converter system are changed, and excellent dynamic performance can be obtained;

- 2). Based on the proposed communication-free power management strategy, when the droop coefficient is changed lags behind the others, and vice versa. This approach provides a possibility for synchronization regulation of the output voltage based on the error between the output phase and the phase average value of all inverters.

- 3). Based on the presented plug-in and plug-out operation for the energy storage unit, the new energy storage unit can be directly plugged in for increasing the power capacity of the energy storage system without reprogramming operation and influencing the dc-link voltage, and the energy storage unit can also be plugged out without obvious impact on the dc-link voltage;

- 4). Combining some existing state of charge balancing methods, the balanced state of change performance of the ESS can be obtained under the proposed communication-free power management strategy. Further, when the centralized man machine interaction system is required for better control performance of the energy storage system, the proposed scheme is easily extended to high-level management system

REFERENCES

- [1] R. H. Lasseter and P. Paigi, "Microgrid: a conceptual solution," in Proc. IEEE Power Electron. Spec. Conf., Jun. 2004, pp. 4285–4290.
- [2] N. Hatziargyriou, H. Asano, R. Iravani, and C. Marnay, "Microgrids," IEEE Power and Energy Magazine, vol. 5, no. 4, pp. 78–94, Jul/Aug. 2007.
- [3] J. Lee et al., "DC micro-grid operational analysis with a detailed simulation model for distributed generation," J. Power Electron., vol. 11, no. 3, pp. 350–359, May. 2011.
- [4] D. E. Olivares, et al, "Trends in microgrid control," IEEE Trans. Smart Grid, vol. 5, no. 4, pp. 1905–1919, Jul. 2014.
- [5] F. Katiraei, M. R. Iravani, and P. W. Lehn, "Micro-grid autonomous operation during and subsequent to islanding process," IEEE Trans. Power Del., vol. 20, no. 1, pp. 248–257, Jan. 2005.
- [6] N. Eghedarpour and E. Farjah, "Control strategy for distributed integration of photovoltaic and energy storage systems in dc micro-grids," J. Renewable Energy, vol. 45, pp. 96–110, Set. 2012.
- [7] S. Lu, L. Wang, T. Lo, and A. V. Prokhorov, "Integration of wind power and wave power generation systems using a dc microgrid," IEEE Trans. Ind. Appl., vol. 51, no. 4, pp. 2753–2761, Jul/Aug. 2015.
- [8] L. Xu and D. Chen, "Control and operation of a dc microgrid with variable generation and energy storage," IEEE Trans. Power Del., vol. 26, no. 4, pp. 2513–257, Oct. 2011.
- [9] K. Sun, L. Zhang, Y. Xing, and J. M. Guerrero, "A distributed control strategy based on dc bus signaling for modular photovoltaic generation

- systems with battery energy storage,” IEEE Trans. Power Electron., vol. 26, no. 10, pp. 3032–3045, Oct. 2011.
- [10] H. Kakigano, Y. Miura, T. Ise, and R. Uchida, “DC micro-grid for super high quality distribution – System configuration and control of distributed generations and energy storage devices –,” in Proc. 37th Annu. IEEE Power Electron. Spec. Conf. (PESC), Korea, 2006, pp. 3148–3154.
- [11] P. Arboleya et al., “Efficient energy management in smart micro-grids: zero grid impact buildings,” IEEE Trans. Smart Grid, vol. 6, no. 2, pp. 1055–1063, Mar. 2015.
- [12] T. Dragicevic, J. M. Guerrero, J. C. Vasquez, and D. Skrlec, “Supervisory control of an adaptive-droop regulated dc microgrid with battery management capability,” IEEE Trans. Power Electron., vol. 29, no. 2, pp. 695–706, Feb. 2014.
- [13] Y. Zhang and Y. W. Li, “Energy management strategy for supercapacitor in droop-controlled dc microgrid using virtual impedance,” IEEE Trans. Power Electron., vol. 32, no. 4, pp. 2704–706, Apr. 2017.
- [14] X. Liu, P. Wang, and P. C. Loh, “A hybrid ac/dc microgrid and its coordination control,” IEEE Trans. Smart Grid, vol. 2, no. 2, pp. 278–257, Jun. 2011.
- [15] P. Sanjeev, N. P. Padhy, and P. Agarwal, “Peak energy management using renewable integrated dc microgrid,” IEEE Trans. Smart Grid, to be published.
- [16] A. G. Tsikalakis, and N. D. Hatziargyriou, “Centralized control for optimizing microgrids operation,” IEEE Trans. Energy Convers., vol. 23, no. 1, pp. 241–248, Mar. 2008.
- [17] J. M. Guerrero, J. C. Vasquez, J. Matas, L. G. De Vicuña, and M. Castilla, “Hierarchical control of droop-controlled ac and dc microgrids—A general approach toward standardization,” IEEE Trans. Ind. Electron., vol. 58, no. 1, pp. 158–172, Jan. 2011.
- [18] S. Moayedi, and A. Davoudi, “Distributed tertiary control of dc microgrid clusters,” IEEE Trans. Power Electron., vol. 31, no. 2, pp. 1717–1733, Feb. 2016.
- [19] J. Park and S. Choi, “Design and control of a bidirectional resonant dc–dc converter for automotive engine/battery hybrid power generators,” IEEE Trans. Power Electron., vol. 29, no. 7, pp. 3748–3757, Jul. 2014.
- [20] S. Sul, “Design of regulators for electric machines and power converters” in Control of Electric Machine Drive System, IEEE Press Series on Power Eng., Piscataway, NJ, USA: Wiley, 2011, pp. 170–173.
- [21] S. Yi, P. W. Nelson, and A. G. Ulsoy, Time-delay systems: Analysis and Control Using the Lambert W Function, Singapore: World Scientific, 2010.
- [22] J. Schönberger, R. Duke, and S. D. Round, “DC-bus signaling: A distributed control strategy for a hybrid renewable nanogrid,” IEEE Trans. Ind. Electron., vol. 53, no. 5, pp. 1453–1460, Oct. 2006.
- [23] X. Lu, et al, “An improved droop control method for dc microgrids based on low bandwidth communication with dc bus voltage restoration and enhanced current sharing accuracy,” IEEE Trans. Power Electron., vol. 29, no. 4, pp. 1800–1812, Apr. 2014.